Polymer Bulletin 33, 361–368 (1994)

**Polymer Bulletin**

© Springer-Verlag 1994

# Fatigue-fracture mechanism of slowly notched poly(ethylene terephthalate) polymers

**J. T. Yeh*, Y. T. Lin, and S. S. Huang**

Graduate School of Textile and Polymer Engineering, National Taiwan Institute of Technology, No. 43, Section 4, Keelung Rd., Tapei, Taiwan

## Summary

Fatigue fracture behavior of slowly notched polyethylene terephathalate (PET) polymers were investigated at temperatures close to their β transition temperatures up to well above their glass transition temperatures. Detailed characterization on the morphology of the notched roots showed that the crack tip during crack propagation became more dull with increasing testing temperature. The failure cycle ($N_f$) of these samples increased with increasing temperatures until it reached the α transition temperatures of PET polymers, and most of the increase in $N_f$ is due to the increased time consumed in the initiation period. On the other hand, the initial crack growth rate increased significantly and $N_f$ of these samples decreased dramatically as the temperature increased well above the glass transition temperature. This interesting temperature dependence of fatigue behavior is explained due to the change of molecular motion of PET polymers at this temperature range.

## Introduction

Influence of testing temperature on dynamic fatigue behavior of polymeric materials have been under investigation for many years (1~9). Most of the publications were concentrated on the studies of amorphous polymers, and the range of testing temperature is generally below their glass transition temperatures. This is probably due to the fact that amorphous polymers become too soft and flexible to use at temperatures above their glass transition temperatures. In contrast, the crystalline polymers remain some degree of mechanical properties even at temperatures well above their glass transition temperatures. However, little information is available in the literature concerning the fatigue properties of the crystalline polymers at temperatures both below and above their glass transition temperatures. For example, as far as we know, no investigation has ever been reported on fatigue properties of polyethylene terephthalate (PET) polymers at temperatures close to or above their glass transition temperatures.

Failure in fatigue mode normally involves an initiation stage before perceivable crack growth can be observed. The initiation is important due to the fact that it may consume a significant portion of the total time to failure. In order to study fatigue crack propagation and its initiation, a notch must be made on the specimens. Although the razor blades are used by many researchers for making the notches, little information is available in the literature about the details of this art. In fact, different notching procedures were often used in the literature, and hence, different microscopic events took place at the root of a notch prior to crack growth, which normally results in poor reproducibility of the initiation data. Therefore, the initiation data associated with these studies are often discarded. In our previous work (10), a clear precrack proceeding the notch tip was found after each PET

*Corresponding author

crystalline sample was notched, and the precrack length became longer when the samples were notched at higher speeds. The failure time ($t_f$) of these samples decreased significantly (Ca. 4 ~ 450 times) when samples were associated with longer precrack lengths, and the percentage of $t_f$ reduced due to faster notching speeds decreased significantly for samples with higher average molecular weight and calculated tie molecule density. Therefore, in order to study the fatigue mechanisms of crystalline PET polymers, a constant and extremely slow notching speed is required to ensure least damage at the root of a notch prior to crack growth, and good reproducibility on the initiation data.

In this work, a constant and extremely slow notching procedure will be used for notching three different molecular weight of polyethylene terephthalate (PET) polymers. The influence of temperature on the dynamic fatigue behavior of polyethylene terephthalate (PET) polymers are investigated at temperatures close to their β transition temperatures up to well above their glass transition temperatures(i.e., the α transition temperatures). A profound effect of temperature on fatigue behavior of PET polymers was found. This interesting temperature dependence of fatigue behavior is explained due to the change of the molecular motion of PET polymers at this temperature range.

## Experimental procedure

### *Materials & sample preparation*

Shinite® PET resins were obtained from Shinkong Synthetic Fibers Corp., Taiwan. Before sample preparation, these resins were dried in a rotational vacuum oven at 150°C for 8 h, cooled at room temperature and maintained in a vacuum desiccator. These dried resins A, B and C, were then injection-molded as rectangular plaques with dimensions of 90 mm x 90 mm x 10 mm and maintained at temperatures 130°C, 130°C and 110°C, respectively, for 2 h. These injection-molded plaques will be referred to as samples A, B and C, respectively. After the required crystallization time, the samples were air cooled. The plaques were then machined into compact-tension specimens (11) with dimensions of 40.0 mm x 38.4 mm x 8.0 mm .

### *Characterization*

*Molecular weight and molecular weight distribution*

The molecular weight and its distribution associated with PET polymers were determined using a Viscotek Gel Permeation Chromatography (GPC) model Sigma 1.0. A liquid-chromatography-precolumn filter was placed in front of the first column to minimize contamination. The samples were prepared by dissolving in pure hexafluoroisopropanol (HFIP) and diluting with chloroform to reach a final concentration of 2 mg/ml in a mixture of chloroform / HFIP (98 : 2 vol %) (12). The amount injected was 0.1 ml; the solvent flow was 1 ml/min at 30°C. Specified molecular weights of narrow fractions of polystyrene were used to calibrate the instrument.

*Thermal analysis*

The melting behavior and the degrees of crystallinity of all samples were studied by using a Dupont differential scanning calorimeter (DSC) model 2000. The degrees of crystallinity of all samples were estimated using baselines drawn from 90 to 280°C and a perfect-crystal heat of fusion of 144 J $g^{-1}$ (13). All scans were carried out at a heating rate of 40°C $min^{-1}$. At least three samples from each specimen type were tested. Lamellar thickness was not measured directly, but was estimated from the observed melting temperature using the Gibbs-Thomson equation (14). Values used in the calculation of lamellar thickness were 1.455 g $cm^{-3}$ for the perfect crystal density (15), 50 erg $cm^{-2}$ for the end-surface free energy (16), and 280°C for the equilibrium melting temperature (16).

*Supermolecular structure and size*

The supermolecular structure of all samples was viewed through crossed polarizer with an Olympus BHSP-300 optical microscope, equipped with an PM-10AK photomicrographic system. Sections 10 μm thick were cut at room temperature from test pieces of PET plaques using a Reichert-Jung Ultracut E Microtome equipped with a glass knife. By drawing lines across the micrograph of each sample, the average sizes of the supermolecular structures can then be calculated as the ratio of the total lengths of the lines to the total numbers of supermolecular structure. Normally, three lines were drawn for each estimation. The spherulite size distributions of these samples represented by the average spherulite size together with its standard deviation.

*Tie molecule density*

In the past, tie molecules have been characterized by using such techniques as transmission electron microscopy (17–24), neutron scattering (25), nuclear magnetic resonance (26), and by measurement of the brittle fracture strength (27). However, due to the small dimensions and complexity of the intercrystalline links, these techniques (excluding the last one) do not appear to be suitable for ready analysis of a relatively large number of bulk samples. In fact, the sensitivity of the method based on brittle fracture stress measurements is also limited in distinguishing samples with relatively small differences in tie molecule density (28). In this study, we used chain dimensions of the polymers to estimate the number of tie molecules formed per chain as suggested recently by Yeh and Runt (28). More detailed description of this method was described in our previous work (10, 28). Although this model is an indirect and qualitative approach for estimating the number of tie molecules, it still allows one to compare and rank a series of samples. As will be seen, these predictions are consistent with the observed changes in mechanical behavior.

***Notching procedure***

Before fatigue experiments, all the compact-tension specimens, prepared as mentioned previously, were initially notched with a hacksaw to a length of 12.8 mm. The notch tip was then made by pressing a fresh razor blade into the inside surface of the specimens until an initial crack length of 13.2 mm was made. The razor blades were pressed at speed of 4 μm $min^{-1}$ at 25°C. A fresh blade was used for each notch.

***Dynamic mechanical testing***

The mechanical relaxation measurements were carried out by means of a dynamic-mechanical analysis (DMA) unit model Eplexor 150 N (GABO Qualimeter Testanlagen GMBH). All DMA experiments were performed at a fixed frequency of 1 Hz and a heating rate of 2°C/min. The temperature ranged from -120°C to 180°C. During measurement, a sinusoidal tensile stress was applied to the samples.

***Fatigue crack propagation***

All fatigue experiments were performed on a Material Test System (MTS) model 810, using a sinusoidal waveform, a minimum-to-maximum load ratio, R, of 0.1 and a frequency of 1 Hz. The MTS machine was equipped with a temperature-controlled chamber with an accuracy of ±0.5°C. In order to obtain the required and an uniform testing temperature on the samples, all specimens were put in the chamber for 30 minutes before fatigue experiments. The maximum loads used for all experiments are 70 kg, 40 kg and 25 kg for samples A, B and C, respectively. Plots of a (the crack length) versus $N$ (fatigue cycle) are used to compare the fatigue behavior obtained from different samples. The stress intensity factor ($K$) for the compact tension specimen was calculated from the applied load ($P$), the specimen thickness ($B$), the distance from the pin loading axis to the back edge of specimen ($W$), and a geometrical factor f(a/W):

$$K = [\, P / (BW^{1/2})] \cdot f(a/W) \qquad (1)$$

where $f(a/W)=\{[2+(a/W)]/[1-(a/W)]^{3/2}\}\cdot[0.886+4.64(a/W)-13.32(a/W)^2+14.72(a/W)^3-5.6(a/W)^4]$(2) and $a$ is the crack length. Plots of $da/dN$ (the crack propagation rate) against $\Delta K$ are used to compare the fatigue behavior obtained from different samples.

## Results and discussion

### *Crystalline Microstructure*

Microstructural characterization of all of the samples is summarized in Table 1. Within experimental error, these samples are associated with approximately same percentage crystallinity, lamellar thickness, average spherulite diameter, but different tie molecule densities. All of samples exhibited the well-known Maltese-cross structure under the polarizing microscope. The average spherulite diameter was around 15 μm. Tie molecule densities predicted from the chain dimensions (10, 28) are 5.66, 5.29, and 3.00 for samples A, B, and C, respectively. This evaluation predicts that the number of tie molecules formed per molecular chain increases with increasing molecular weight, which qualitatively agrees with expectation from literatures(10, 18, 27, 28).

Table 1 Microstructural characterization

| Sample | Mw | Percentage crystallinity (%) | Average spherulite diameter (μm) | Lamellar thickness (nm) | Tie molecule density |
|---|---|---|---|---|---|
| A | 7.5E4 | 46 | 15±1 | 8.8 | 5.66 |
| B | 6.8E4 | 46 | 15±3 | 8.9 | 5.29 |
| C | 4.6E4 | 46 | 15±2 | 8.9 | 3.00 |

### *Dynamic Mechanical Analysis*

The temperature dependence of the loss of tangent δ for samples A, B, and C is shown in Fig.1. No significant difference was found in the nature of these curves, two distinct transitions were observed as tanδ peaks at temperatures near -47°C (β transition) and 93°C(α transition) in all of these three curves. The two transition processes of poly(ethylene terephthalate) have been the subject of many previous investigations (29-31). There is some doubt about the molecular origins of the α and β relaxation, however, it is generally agreed that the α relaxation consists of micro-Brownian motions of the chain, and a composite process involving more restricted motions of specific portions of the chain is accounted for the β relaxation. Farrow et al. (30) concluded that the α relaxation involves considerable motion of both the -O-$CH_2$-$CH_2$-O- residue and the *p*-phenylene linkages in the amorphous regions. On the other hand, a very restricted degree of molecular mobility (probably only in the glycol residue) is associated with the β relaxation. Illers and Breuer (31) suggested that the β relaxation could be resolved into three separate processes. The two higher-temperature processes were thought to involve motion of carboxyl groups. The low-temperature process was considered to be caused by the motion of the -$C_2H_4$- unit.

### *Fatigue - Fracture Mechanism*

#### *Notched root morphology*

Typical morphology of the notched root of sample A during fatigue crack propagation (FCP) process is shown in Figs. 2-6. The crack tip became more dull with increasing testing temperature. Similar temperature dependence of the morphology of the notched root of samples B and C was also observed.

#### *Fatigue Crack Propagation*

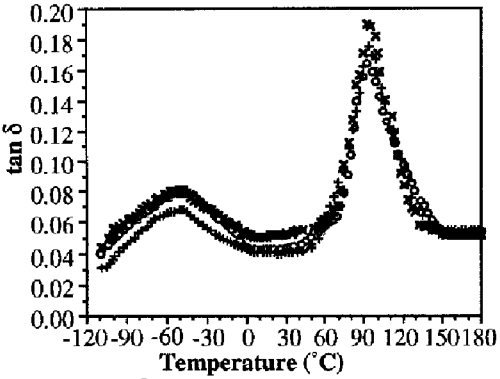


Figure 1 tanδ plotted against testing temperatures at 1Hz for samples A (o), B (+), and C (x).

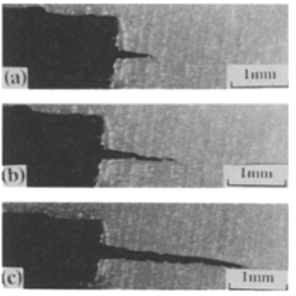


Figure 2 Optical micrographs of the notched root morphology of sample A at -20°C: (a) 1858 cycles, (b) 2304 cycles, (c) 2601 cycles.

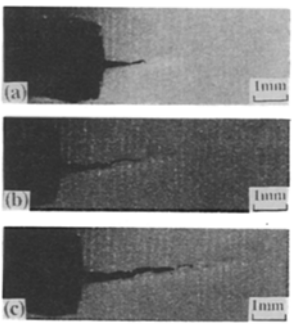


Figure 3 Optical micrographs of the notched root morphology of sample A at 0°C: (a) 3865 cycles, (b) 4458 cycles (c) 4982 cycles.

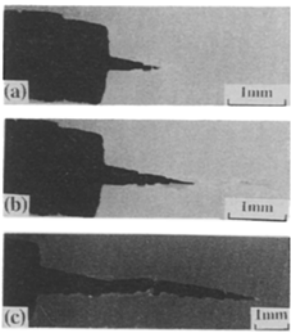


Figure 4 Optical micrographs of the notched root morphology of sample A at 25°C: (a) 9851 cycles, (b) 10301 cycles, (c) 12165 cycles.

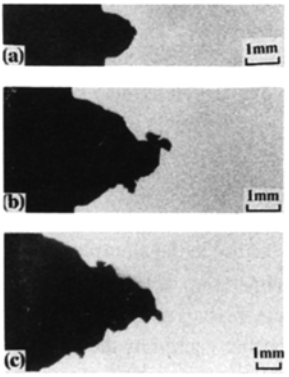


Figure 5 Optical micrographs of the notched root morphology of sample A at 75°C: (a) 5565 cycles, (b) 17844 cycles, (c) 20268 cycles.

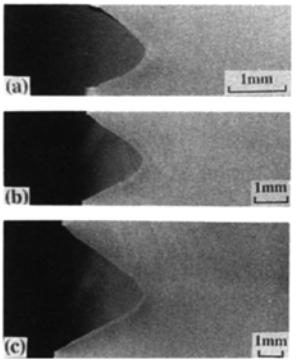


Figure 6 Optical micrographs of the notched root morphology of sample A at 130°C: (a) 15 cycles, (b) 39 cycles, (c) 46 cycles.

Plots of crack growth rate (da/dN) against the stress intensity factor (ΔK) of samples A, B, and C are shown in Fig. 7. A higher FCP resistance was observed at each testing temperature for samples associated with higher tie molecule density and weight average molecular weight ($M_w$) (i.e., from C to A ). Similar tie molecule density (or $M_w$ ) dependence of FCP resistance of other crystalline polymers has been reported before (28, 32-36).

Table 2 summarized the average fatigue-failure cycle associated with each sample tested at varying temperatures. At least three fatigue crack propagation experiments were performed at each testing condition. By focusing on sample A first, it is interesting to note that the failure cycle ($N_f$) increased with increasing temperatures until it reached the α transition temperature of sample A. In contrast, $N_f$ of sample A decreased dramatically with increasing temperature as the temperature (i.e., 130°C) increased well above its α transition temperature. Similar temperature dependence of $N_f$ was also observed for samples B and C. (see Table 2)

Plots of crack length (a) against fatigue cycle (N) of samples A, B, and C tested at various temperatures are shown in Fig.8. As shown in these plots, an initiation period ($N_i$) is observed at temperatures below their α transition temperatures (see Fig. 8a), at which the crack growth rate is very slow. After the initiation period, the crack grows stably and faster than those grown in the initiation period before catastrophic failure occurs. In fact, it is interesting to note that most of the increase in $N_f$ with increasing temperature is due to the increased time consumed in the initiation period, and the time consumed after the initiation period is approximately the same for all samples tested at temperatures below their α transition temperatures. On the other hand, the initial crack growth rate increased significantly as the temperature raised to close to and above their α transition temperature, and the demarcation between the initiation and stable crack growth regions became obscured. Consequently, the samples became too soft to undergo stable crack growth, and failured in a short period as the temperature raised well above their α transition temperatures.

Presumably, it is generally believed that FCP resistance and $N_f$ decrease as the molecular motion becomes more active, because disentanglement of polymer chains during FCP process can be enhanced with active molecular motion, which is often encountered with increasing temperature. It is, therefore, a significant increase in the initial growth rate was observed at temperatures raised to close to or above the α transition temperatures of PET polymers. However, as mentioned previously, the crack tip became duller with increasing temperature, which may result in a lower stress concentration at the crack tip, a higher FCP resistance and longer $N_f$. It is not completely clear at this point what role does the molecular motion can play in determining the fatigue-fracture mechanisms of PET polymers at different temperature ranges. However, one possible rationale is described as follows. As mentioned previously, Farrow et al. (31) suggested that "completely" molecular motion in the amorphous regions does not occur at temperatures between the α and β transition temperatures of PET polymers, since the considerable motion of both the -O-$CH_2$-$CH_2$-O- residue and the *p*-phenylene linkages of main-chain molecules in the amorphous regions do not rotate completely at temperatures below the α transition temperature of PET polymers. It may be, therefore, only slight increase in the molecular motion with increasing temperatures, which may not be enough to compensate the beneficial effect on FCP resistance caused by the duller crack tips of samples tested at higher temperatures. Therefore, $N_f$ and the cycles spent in the initiation period ($N_i$) increase with increasing temperature at temperatures below the α transition temperatures of PET polymers. However, "completely" molecular motion occurs in the amorphous region at temperatures well above the α transition temperature , which may dramatically increase the initial

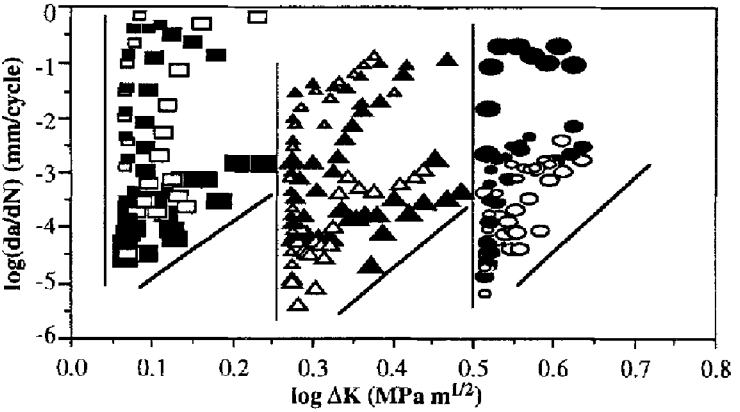


Figure 7 Crack growth rate (da/dN) plotted against stress intensity factor (ΔK) for samples A at -20°C (●), 0°C(○), 25°C(●), 75°C(○), 130°C(●), samples B at -20°C (▲), 0°C(△), 25°C(▲), 75°C(△), 130°C(▲), samples C at -20°C (■), 0°C(□), 25°C(■), 75°C(□), 130°C(■).

Table 2 The average fatigue-failure cycle associated with each sample tested at varying temperatures.

| failure cycles($N_f$) / sample / testing temperature | A | B | C |
|---|---|---|---|
| -20°C | 2743 | 1802 | 60 |
| 0°C | 5452 | 5426 | 106 |
| 25°C | 13233 | 14088 | 9144 |
| 75°C | 21521 | 68903 | 18708 |
| 130°C | 52 | 39972 | 13934 |

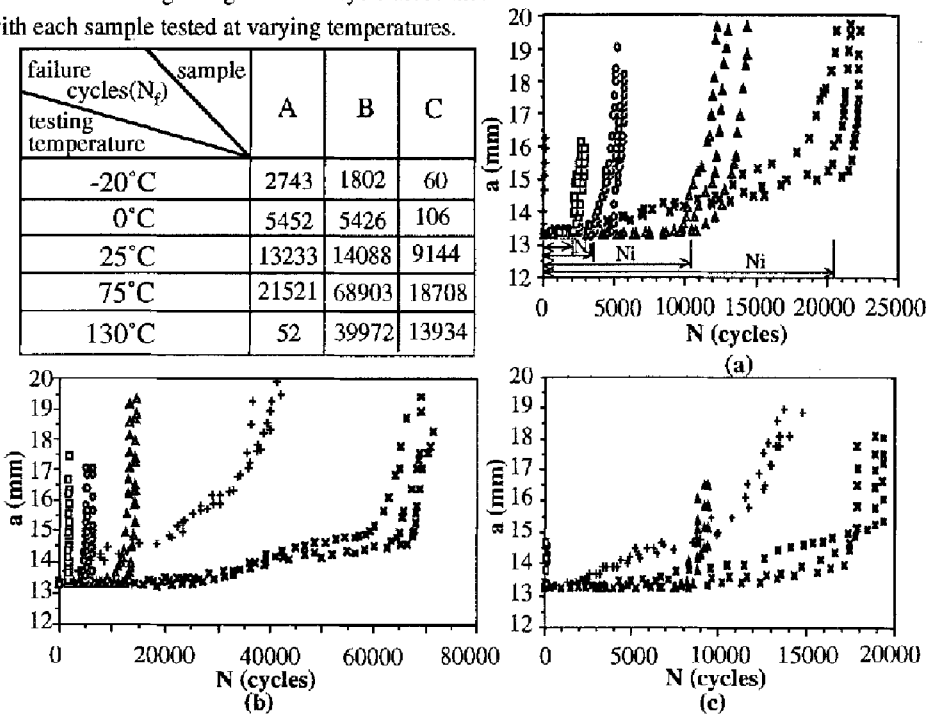


Figure 8 Crack length (a) plotted against fatigue cycle (N) at 130°C(+), 75°C(x), 25°C(Δ), 0°C(o), -20°C(□) for samples (a) A, (b) B, and (c) C.

crack growth rate possibly by disentanglement of polymer chains. Therefore, $N_f$ decreased significantly even though a dulled crack tip was still observed at temperatures well above the $\alpha$ transition temperatures of PET polymers.

**References**


1. Kurobe T and Wakashima H (1970) Jpn. Congr. Mater. Res. – Non-Metall. Mater., 13: 192
2. Kurobe T and Wakashima H (1972) Jpn. Congr. Mater. Res. – Non-Metall. Mater., 15: 137
3. Radon JC and Culver LE (1975) Polym. Eng. Sci., 15(7): 500
4. Skibo MD, Ph. D. Dissertation (1977) Lehigh Univ.
5. Cheng WM, Miller GA, Manson JA, Hertzberg RW, and Sperling LH (1990) J. Mater. Sci., 25: 1924
6. Mai YM and Williams JG (1979) J. Mater. Sci., 14(8): 1933
7. Martin GC and Gerberich WW (1976) J. Mater. Sci., 11: 231
8. Wann RJ, Martin GC, and Gerberich WW (1976) Polym. Eng. Sci., 16(9): 645
9. Gerberich WW and Martin GC (1976) J. Polym. Sci., Polym. Phys. Ed., 14: 897
10. Yeh JT, and Lin YT (1993) J. Mater. Sci., 28: 3900
11. Plane-Strain Fracture Toughness of Metallic Materials (1989) ASTM E399-83
12. Weisskopf K (1988) J. Polym. Sci., Part A, 26:1919
13. Slade PE, Orfino TA (1968) in Analytical Calorimetry, eds. Porter RS, Johnson JF, p.63
14. Hoffman JD, Davis GT and Lauritzen JI (1975) "Treatise on Solid State Chemistry", vol. 3, edited by Hannyay NB
15. Daubeny RP, Bunn CW, Brown CJ (1954) Proc. Roy. Soc., London, A226: 531
16. Alfonso GC, Pedemonte E and Ponzetti L (1979) Polymer, 20: 104
17. Keith HD, Padden FJ, and Vadimsky (1966) J. Polym. Sci., Part A-2, 4: 267
18. Keith HD, Padden FJ, and Vadimsky RG (1966) J. Appl. Phys., 37: 4027
19. Keith HD, Padden FJ, and Vadimsky RG (1971) J. Appl. Phys., 42: 4585
20. Vadimsky RG, Keith HD, and Padden FJ (1969) J. Polym. Sci., Part A-2, 7: 1367
21. Davis HA (1966) J. Polym. Sci., Part A-2, 4: 1009
22. Nagou S and K Azuma (1979) J. Macromol. Sci., Phys. Ed., 16: 435
23. Clark ES (1967) S. P. E. J., 23: 46
24. Keith HD, Padden FJ, and Vadimsky RG (1980) J. Polym. Sci., Polym. Phys. Ed., 18:2307
25. Fischer EW, Hahn K, Kugler J, and Struth U (1984) J. Polym. Sci., Polym. Phys. Ed., 22: 1491
26. Zhizhenkov VV and Egorov EA (1984) J. Polym. Sci., Polym. Phys. Ed., 22: 117
27. Brown N and Ward IM (1983) J. Mater. Sci., 18: 1413
28. Yeh JT and Runt J (1991) J. Polym. Sci., Polym. Phys. Ed., 29: 371
29. Mccrum NG, Read BE, and Williams G (1967) Anelastic and Dielectric Effects in Polymeric Solids, Wiely, New York-London
30. Fallow G, Mcintosh J, and Ward IM (1960) Makromol. Chem., 38: 147
31. Illers KH and Breuer H (1963) J. Collid. Sci., 18: 1
32. Yeh JT and Runt J (1989) J. Mater. Sci.,24: 2637
33. Sauer JA, Foden E, and Morrow DR (1977) J. Polym. Eng. Sci., 17: 246
34. Ramirez A, Manson JA, and Hertzberg RW (1982) Polym. Eng. Sci., 22: 975
35. Charentenay FX, Laghouati F, and Dewas J (1979) in Deformation, Yield and Fracture of polymers, Plastics and Rubber Institute, London, p.61
36. Bretz PE, Manson JA, and Hertzberg RW (1982) J. Appl. Polym. Sci., 27: 1707


Accepted May 30, 1994 Shi